IEEE Access
Multidisciplinary : Rapid Review : Open Access Journal

Received May 21, 2020, accepted June 5, 2020, date of publication June 11, 2020, date of current version June 29, 2020.

Digital Object Identifier 10.1109/ACCESS.2020.3001658

Fuzzy Mapped Histogram Equalization Method for Contrast Enhancement of Remotely Sensed Images

MOHAMMAD FARHAN KHAN[1], EKRAM KHAN[2], MUAFFAQ M. NOFAL[3], AND M. MURSALEEN[4,5,6]

[1]Department of Electrical Engineering, IIT Roorkee, Roorkee 247667, India
[2]Department of Electronics Engineering, Aligarh Muslim University, Aligarh 202002, India
[3]Department of Mathematics and General Sciences, Prince Sultan University, Riyadh 11586, Saudi Arabia
[4]Department of Medical Research, China Medical University Hospital, China Medical University, Taichung 40402, Taiwan
[5]Department of Computer Science and Information Engineering, Asia University, Taichung 41354, Taiwan
[6]Department of Mathematics, Aligarh Muslim University, Aligarh 202002, India

Corresponding author: M. Mursaleen (mursaleenm@gmail.com)

ABSTRACT Histogram equalisation (HE) is a widely used image contrast enhancement technique which is less computationally complex, but it fails to preserve the brightness and natural appearance of the remotely sensed images. To overcome these limitations several modifications have been reported in the literature. However, the images processed by most of the methods still suffer with the problems of saturation artifacts and un-even expansion of intensities. This paper proposes a novel fuzzy mapped HE method to overcome the aforementioned limitations by partitioning the histogram into multiple segments, expanding each segment to full dynamic range using fuzzy mapping function, then equalising each segment independently, and finally normalising the combination of equalised segments. The normalisation process is controlled by a non-negative control factor, which requires a training data for its estimation. Experimental results demonstrate that the application of proposed method in the area of remote sensing yields better results than the contemporary methods.

INDEX TERMS Histogram equalization, saturation artifacts, un-even expansion of intensities, fuzzification.

I. INTRODUCTION

The real-world applications such as remote sensing, astronomy, military etc. generally use high resolution (HR) images carrying enormous amount of minuscule data that plays a significant role in interpreting the information correctly [1], [2]. Although the remote sensing devices equipped with HR cameras record image/video with appropriate geometric and radiometric corrections, but may not be sufficient to deliver an image with desirable brightness and contrast [3]–[6]. The images received at the earth station might not be visually pleasing due to undesirable atmospheric conditions such as haze, fog, excess darkness etc. The dynamic range of intensity of images under extreme weather conditions is generally much narrower than its desirable value, which largely impacts the visibility of such poor contrast images. The information extracted from such images is limited because of insufficient visual perception of the images. Hence, it is vital to enhance the image contrast, so that the visual appearance of the image can be improved for accurate interpretation and understanding.

Among various contrast enhancement techniques, linear stretching (LS) and histogram equalisation (HE) are most effective, low cost and widely used techniques. LS technique achieves contrast enhancement by stretching the image histogram across the permissible dynamic range, but it fails to enhance the images that contains low peak regions across the extreme edges of the histogram. The piecewise LS (PLS) method overcomes this problem, but it needs manual selection of parameters for section determination, hence can't be used in automated systems [7]. Recently, histogram compaction transform with local linear stretching (HCTLS) method has been proposed to remove the small regions from image histogram and uses dual gamma correction on dark and bright regions [7].

On the other hand, HE methods achieve overall contrast enhancement by stretching the dynamic range of the image histogram using cumulative distribution function (cdf) as a

The associate editor coordinating the review of this manuscript and approving it for publication was Ikramullah Lali.

mapping function [8]. In terms of thresholding, HE techniques are broadly classified in three categories, namely conventional HE (CHE or uni-HE), bi-HE, and multi-HE. Note that, the CHE method acts as a core of bi-HE and multi-HE methods. CHE method expands the standard deviation of the image to larger extent, but unable to preserve the mean brightness and natural appearance of output image due to over enhancement [9]. The undesirable artifacts observed in CHE method have been minimised by advanced HE methods, which divides the input image histogram into either two (termed as bi-HE) or more than two (termed as multi-HE) non-overlapping segments, and then equalise each segment independently.

Among bi-HE methods, brightness preserving bi-HE (BBHE) [9] is one of the earliest work that partitions the histogram into two segments before equalising the segments. Recently bi-HE using modified histogram bins (BHEMHB) method has been suggested [10], which integrates the histogram segmentation process with the modification of histogram bins. Compared to CHE method, both BBHE and BHEMBE methods are able to significantly control the equalisation process. The recursive mean based HE (RMSHE) method [11] that divides the histogram into more than two segments by applying BBHE method recursively is a classical yet popular multi-HE method. However, the multi-HE methods fail to prevent the excessive saturation of intensity bins causing the visual artifacts and loss of natural appearance in the processed images.

To overcome the limitation of un-even expansion of intensity bins in classical multi-HE methods, several crisp and soft computing based algorithms have been introduced which either defines the target metric to control the enhancement process or pre-process the original histogram before equalisation process [12]. Along with crisp HE methods, the fuzzy based HE algorithms have also been utilised to preserve the brightness and natural appearance of the images. Most of the fuzzy based HE methods either transform the crisp histogram into fuzzy histogram before segmentation process or utilises fuzzy logic for segmenting the crisp histogram into sub-histograms before enhancement process [8], [13], [14].

This paper proposes a fuzzy based HE technique that transforms the SDDMHE method [12] by mapping each segment in a way that it can achieve maximum expansion of bins during equalisation process without encountering the saturation problem. The algorithm transforms each segment to the new dimension with the help of a fuzzy mapping function and then applies HE over each sub-histogram individually. The proposed idea is based on the fact that, compared to crisp expansion, the fuzzification of intensities provide more degree of flexibility in the expansion process, therefore reducing the chances of overlapping of intensities.

The reminder of the paper is as follows: Section II presents the histogram equalisation method using fuzzy maximal dynamic expansion. The comparison of results of various HE methods are discussed in Section III. Finally, the paper is concluded in section IV.

II. PROPOSED METHOD

Consider an image I, having $[X_l, X_u]$ intensity levels (where X_l and X_u is lower and upper intensity level respectively). The cdf at k^{th} intensity level (X_k) can be defined as:

$$c(X_k) = \sum_{q=X_0}^{X_k} \frac{n_q}{N} \qquad \forall X_k \in \{X_0, X_{L-1}\} \tag{1}$$

where, n_q is the number of pixels whose intensity value is less than or equal to X_q, N is the total number of pixels in the image, and $L = 256$ for 8 bit image. The mapping function for k^{th} intensity level, can be obtained from the input cdf as:

$$T(X_k) = |X_{L-1} \times c(X_k)| \tag{2}$$

where, $|x|$ is the integer nearest to x. Note that, the value of $c(X_{L-1})$ is unity. The output image O, can be obtained by:

$$O(i, j) = T[I(i, j)] \qquad (i, j) \in I \tag{3}$$

The proposed method relies on the fact that the expansion of intensity levels by HE on each segment plays an important role in preservation of natural appearance of the images. If the sub-histograms opted for equalisation process is narrow, then the equalised intensities will saturate over each other, resulting into visual artifacts in the processed images. The proposed method partitions the input histogram into four sub-histograms (or segments) using mean intensity as thresholds, similar to RMSHE with $n = 4$. Then each segment is expanded to the full intensity range $[X_0, X_{L-1}]$ using fuzzy mapping function. It may be noted that, $n = 4$ is selected as trade-off value to preserve the brightness as well as to guarantee the less saturation artifacts by avoiding unessential increase in the computational complexity of the algorithm [12].

Let input histogram $H[X_l, X_u]$ is partitioned into n non-overlapping segments, such that

$$H[X_l, X_u] = \bigcup_{r=1}^{n} H_r[X_l^{r,n}, X_u^{r,n}] \tag{4}$$

where, H_r denotes r^{th} segment with $X_l^{r,n}$ and $X_u^{r,n}$ as lower and upper boundaries respectively. Note that $X_l^{1,n} = X_0$ and $X_u^{n,n} = X_{L-1}$. It is worthy to note that, intensity overlapping or saturation during the enhancement process using LS, HE is a common problem that need to be countered efficiently. Otherwise it might lead to loss of information or negative extraction of information. This is particularly important in remote sensing images. The proposed fuzzy expansion process is somewhat similar to PLS, but with fully automated histogram stretching process. It is this step where proposed algorithm differs with other competing HE methods.

The purpose of using fuzzy membership function is to provide randomness into the mapped sub-histograms of the image. It has been observed that during the equalisation process, the high probability regions of the histogram overlaps with low probability regions, which is one of the sources of visual artifacts and loss of information content in the processed images [12]. In order to avoid the this overlapping, the sub-histograms can be mapped to new fuzzy levels instead

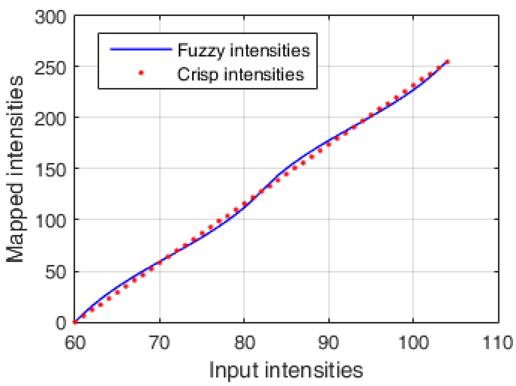

FIGURE 1. Demonstration of fuzzy mapping with respect to linear crisp mapping of gray level intensities for the sample sub-histogram constituting random 44 gray scale levels ranging between [60], [104].

of linearly separated crisp levels. The fuzzification of intensities provides more levels for expansion that slays down the probability of overlapping of intensities compared to crisp expansion of intensities.

Let intensity level X_k of r^{th} segment is to be mapped to new fuzzy intensity level (X_{kf}) which can be determined from (5).

$$X_{kf} = \begin{cases} \dfrac{X'_k \times X'_{L/2} \times (2X'_k - 3)}{4{X'_k}^2 - 2X'_k - 1} & \text{if } X'_k \in \left[{X'_l}^{r,n}, {X'_u}^{r,n}/2\right) \\ \dfrac{X'_{L/2} \times (2X'_k - 3) \times (3X'_k - 1)}{4{X'_k}^2 - 6X'_k + 1} & \text{if } X'_k \in \left[{X'_u}^{r,n}/2, {X'_u}^{r,n}\right] \end{cases} \tag{5}$$

where, $X'_k = X_k/{X'_u}^{r,n}, X_k \in \mathbb{W}$ is the original crisp intensity level of the image, ${X'_l}^{r,n} = X_l^{1,n}, {X'_u}^{r,n} = {X_u}^{r,n} - X_l^{r,n}$ and $X_{kf} \in \mathbb{R}$ is the fuzzy mapped intensity level. Fig. 1 demonstrates the role of fuzzy mapping in transforming the gray scale levels into fuzzy levels. From Fig. 1, it can be asserted that the fuzzy mapped intensities are able to transformed grey level intensities $X_k \in \mathbb{W}$ to $X_{kf} \in \mathbb{R}$ without largely disturbing the behaviour as that of linear crisp stretching.

After stretching the image histogram to new fuzzy intensities, CHE technique is used to equalise each segment independently. The equalised segments are then added together to construct an enhanced image. Further, the defuzzification or normalisation of intensity levels of the output image is performed, which transfers the fuzzified intensities back to crisp intensities lying in the range $[0, L-1]$. The normalised intensity (X''_k) is the weighted average of corresponding intensity of input and processed image.

$$X''_k = \left| \frac{(w_{min} \times X_k) + T_c(X_{kf})}{w_{min} + 1} \right| \tag{6}$$

where, $T_c(X_{kf})$ is the fuzzy intensity produced after combining all equalised sub-images, and w_{min} is a non-negative weight. Two image features namely, entropy (E) (defined in Eqn. 7) and universal image quality (UIQ) (defined in Eqn. 8) are used to determine the value of w_{min} [15]. These features are the measure of information content and perceived quality of enhanced image $O(i,j)$ respectively. The low value of E and UIQ in enhanced image may result due to the saturation of intensities during enhancement process, and is undesirable in remotely sensed images. The value of w_{min} is selected such that E and UIQ of the normalised output image $O(i,j)$ are maximised.

The entropy of the output image ($O(i,j)$) can be defined as:

$$E = -\sum_{k=0}^{L-1} p(X''_k) \times \log_2 p(X''_k) \quad \text{(bits)} \tag{7}$$

where, $p(X''_k)$ is the probability of kth intensity level in enhanced image $O(i,j)$. Similarly, UIQ is defined as:

$$UIQ = \frac{4\sigma_{IO} \times m(I) \times m(O)}{(\sigma_I^2 + \sigma_O^2)[(m(I))^2 + (m(O))^2]} \tag{8}$$

where, $m(I)$ and $m(O)$ are mean brightness of input and output images respectively, σ_I^2 and σ_O^2 are variance of intensity in input and output images respectively. These parameters and σ_{IO} are defined as follows:

$$\sigma_I^2 = \frac{1}{N-1}\sum_{i=1}^{N}(I_i - m(I))^2, \sigma_O^2 = \frac{1}{N-1}\sum_{i=1}^{N}(O_i - m(O))^2$$

$$\sigma_{IO} = \frac{1}{N}\sum_{i=1}^{N}(I_i - m(I))(O_i - m(O))$$

where, N is the total number of pixels in the image. To determine the optimal value of w_{min}, it's value is calculated for each of the 30 training images and then averaged. The characteristics of data sets are listed in Table 1. The optimal value of w_{min} is obtained as follows. Let w_1 and w_2 are the weights used to optimize entropy (E) and universal image quality (UIQ) of output image $O(i,j)$. The process starts by initializing the values of w_1 and w_2 to zero and increasing them at the constant step, and corresponding values of E and UIQ are recorded. The process continues until the values of E and UIQ saturates and change in corresponding values are zero. The minimal value of w_1 and w_2 at which E and UIQ are correspondingly maximized are noted as w_{min_E} and $w_{min_{UIQ}}$ respectively. The optimal weight w_{min} is then obtained by averaging w_{min_E} and $w_{min_{UIQ}}$, the weights that optimize E and UIQ individually. The process of determining w_{min} can be mathematically written as:

$$w_{min_E} = \min(w_1) | E \text{ is maximum} \tag{9}$$

$$w_{min_{UIQ}} = \min(w_2) | UIQ \text{ is maximum} \tag{10}$$

$$w_{min} = \frac{w_{min_E} + w_{min_{UIQ}}}{2} \tag{11}$$

The execution time for estimating the value of w_{min} is 317 seconds. The average error associated with the training data can be estimated in terms of entropy error (i.e. difference between input entropy and output entropy) and inverse UIQ (i.e. $1 - UIQ$), the respective values are 0.07 bits and 0.015.

TABLE 1. Characteristics of ID1, ID2 images and average data sets.

Image ID	Mean	E(bits)	Dimension
ID1	77.38	5.75	1550 ×1547
ID2	138.48	6.73	1024×1024
Training set (30 images)	131.24	6.49	-
Testing set (100 images)	139.61	6.75	-

The proposed method can easily be extended to the colour images by transforming the RGB image into luminance-chrominance colour spaces such as HSV, CIE $\mathbb{L}*a*b$, HSI etc., and applying the proposed algorithm to the luminance component $\mathbb{L}*$ or V only. The chrominance components are left untouched. Finally, the inverse transformation with equalized luminance component and original chrominance components is applied to get back the enhanced RGB image.

III. RESULTS AND DISCUSSION

A data set of 100 high altitude aerial test images including 30 training images are used to compare the performance of proposed method with other contemporary methods. These images have been taken from the USC's SIPI image database (http://sipi.usc.edu/database/database.php?volume=aerials) and Inria aerial image database having spatial resolution of 0.3m [16]. In order to visualise the impact of contrast enhancement algorithm, the standard deviation of all the sample images has been reduced from its original value.

In this section, the qualitative and quantitative assessments of only two images (ID1 and ID2) are presented here. Also, the average performance (averaged over all 100 test images) of proposed method is evaluated and compared with other state-of-the-art methods such as CHE, BBHE [9], BPDFHE [13], SDDMHE-M ($n = 4$) [12], BHEMHB [10], RMSHE ($n = 4$) [11] and Fuzzy segmented HE ($l^- = 0.1349$ and $l^+ = 0.2481$) [8]. For the proposed method, $n = 4$ and $w_{min} = 18.2$ are used. All experiments have been simulated in MATLAB R2013b on a PC equipped with 8.0 GB RAM and Intel Core i5 1.80GHz CPU.

The histograms of images ID1 and ID2 have very narrow dynamic range (low contrast), either due to insufficient light source or covered with haze, thereby affecting the visibility of the region. As the human perception mechanisms are very sensitive to the edges, the compression of visual dynamic range reduces the subjective clarity of the image because the intensity of pixels surrounding the edges have smaller variance. The contrast of such images can be efficiently enhanced by widening the differences among the intensity bins surrounding the edges of the image. The rarefaction of the bins is possible by utilising the cdf of the image.

Fig. 2 shows the subjective comparison among different HE algorithms for ID1 image captured during insufficient light source. By observing these images, it can be stated that the proposed method performs efficiently and the image processed by proposed method is evenly enhanced similar to that of SDDMHE-M method. Although the gray scale expansion of histogram by SDDMHE-M has less saturation artifacts than the proposed method, extreme edges of the histogram clearly fail to capture the complete dynamic range of the gray scale; thereby making the histogram equalisation process relatively cumbersome. Whereas, the other HE methods have changed the original characteristics of the image histogram to larger extent. This change in characteristics is mainly due to the problem of saturation of intensities, which is undesirable. Therefore, it can be concluded that the proposed method not only reduces saturation artifacts, it also utilises the complete dynamic range for improved visibility of processed image. Note that, the zoom-in version of region of interest are given in appendix for better interpretation.

A close observation of Fig. 3 reveals that the ID2 image processed by CHE, BBHE and Fuzzy HE methods suffer with over enhancement of mid region while saturating the extreme regions, while BPDFHE, RMSHE and BHEMHB methods have produced images of high brightness. That is, most of the methods suffer from over or under enhancement in various histogram regions. On the other hand, SDDMHE-M and the proposed methods give almost similar quality output image, but the histogram of the image of SDDMHE-M do not covers the complete dynamic range of intensities. Observing the floral designed floor on the extreme left of the pentagon, it can be stated that the proposed method has utilised the visual dynamic range of the image more efficiently than SDDMHE-M (or any other contemporary) method by expanding the intensities of sub-histograms to full dynamic range with the help of fuzzy mapping function.

For quantitative comparison, five performance metrics namely peak signal to noise ratio (PSNR), UIQ, image quality measure rating (R) [17], absolute mean brightness error (AMBE), and E are used. Table 2 lists the values of all these metrics for images ID1 and ID2, as well as average values for 100 test images. Among the five considered metrics, three metrics namely PSNR, UIQ, and R measure the visual quality of the output images. Ideally, the value of UIQ and R should be unity and zero respectively, whereas high value of PSNR signifies better preservation of natural appearance. AMBE measures the brightness preservation characteristics, whereas entropy E is the measure of information richness in the output image. Note that, in Table 2 the best performing metric for average performance is highlighted with boldface.

By observing Table 2, it can be concluded that the proposed method preserves the natural appearance of the ID1 and ID2 images quite effectively and outperforms other contemporary methods in terms of PSNR and UIQ. Although the value of R of the proposed method for ID2 image is not considerably large but lies very close to that of SDDMHE-M method. Furthermore, the value of AMBE for proposed method for ID1 and ID2 images is 9.57 and 4.82 respectively is again little bit higher than that of SDDMHE-M but quite close to it, which indicates effective brightness preservation characteristic of the proposed method. It can also be observed from Table 2 that the proposed method has high value of E, which are quite close to that of input images, signifying the information richness of the output image. Table 2

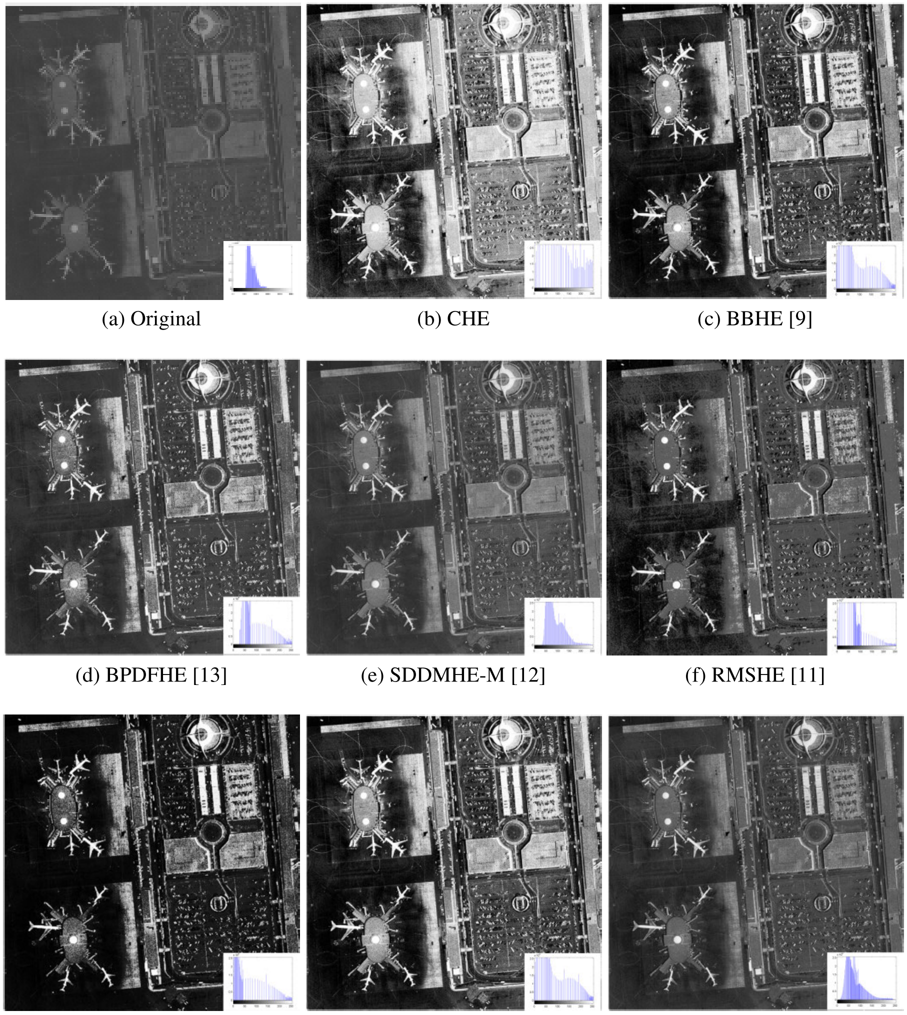

(a) Original (b) CHE (c) BBHE [9]

(d) BPDFHE [13] (e) SDDMHE-M [12] (f) RMSHE [11]

(g) BHEMHB [10] (h) Fuzzy segmented HE [8] (i) Proposed

FIGURE 2. Results of various HE methods for ID1 image with respective histograms with respect to original image.

TABLE 2. Comparison of various HE methods for ID1, ID2 images and average of 100 test images in terms of PSNR, *UIQ*, *R*, AMBE, *E* and computation time.

Metrics	HE methods											
	CHE			BBHE [9]			BPDFHE [13]			SDDMHE-M [12]		
	ID1	ID2	Avg.	ID1	ID2	Avg.	ID1	ID2	Avg.	ID1	ID2	Avg.
PSNR	10.42	14.25	15.86	15.54	19.68	18.05	20.73	21.97	22.27	29.79	31.94	30.41
UIQ	0.584	0.732	0.608	0.692	0.779	0.746	0.816	0.893	0.819	0.907	0.928	0.953
$R(\times 10^{-4})$	76.29	8.69	54.95	57.27	7.82	30.46	38.15	7.27	21.03	7.62	3.32	5.24
AMBE	50.64	11.03	33.29	28.13	9.30	16.96	17.39	8.14	13.65	8.01	3.96	**6.40**
E	4.02	5.64	5.68	4.47	6.41	6.41	4.51	6.38	6.48	5.66	6.69	**6.71**
Time	2.18	0.94	**1.26**	4.59	1.97	2.63	6.97	2.99	3.95	7.38	3.21	4.29
Metrics	HE methods											
	RMSHE [11]			BHEMHB [10]			Fuzzy segmented HE [8]			Proposed		
	ID1	ID2	Avg.	ID1	ID2	Avg.	ID1	ID2	Avg.	ID1	ID2	Avg.
PSNR	18.53	20.61	23.08	19.81	22.98	24.06	15.21	19.35	17.98	30.73	32.41	**31.68**
UIQ	0.736	0.877	0.831	0.791	0.848	0.832	0.703	0.762	0.758	0.924	0.936	**0.961**
$R(\times 10^{-4})$	25.02	6.68	23.86	29.44	9.23	11.34	55.96	8.01	29.92	4.76	3.37	**3.06**
AMBE	18.09	5.07	10.04	19.03	14.64	10.25	27.83	9.01	17.08	9.57	4.82	6.94
E	4.57	6.25	6.52	4.29	6.01	6.23	4.39	6.38	6.35	5.52	6.67	6.63
Time	5.47	2.38	3.19	7.03	2.61	3.29	7.20	3.76	5.01	8.23	3.57	4.71

also includes the value of parameters averaged over 100 test images and their execution time (in seconds). It can be observed that, out of five metrics, the proposed method outperforms in three metrics on the average basis. Although the execution time of the proposed algorithm is higher than that of CHE, but still close to that of BPDFHE and SDDMHE-M

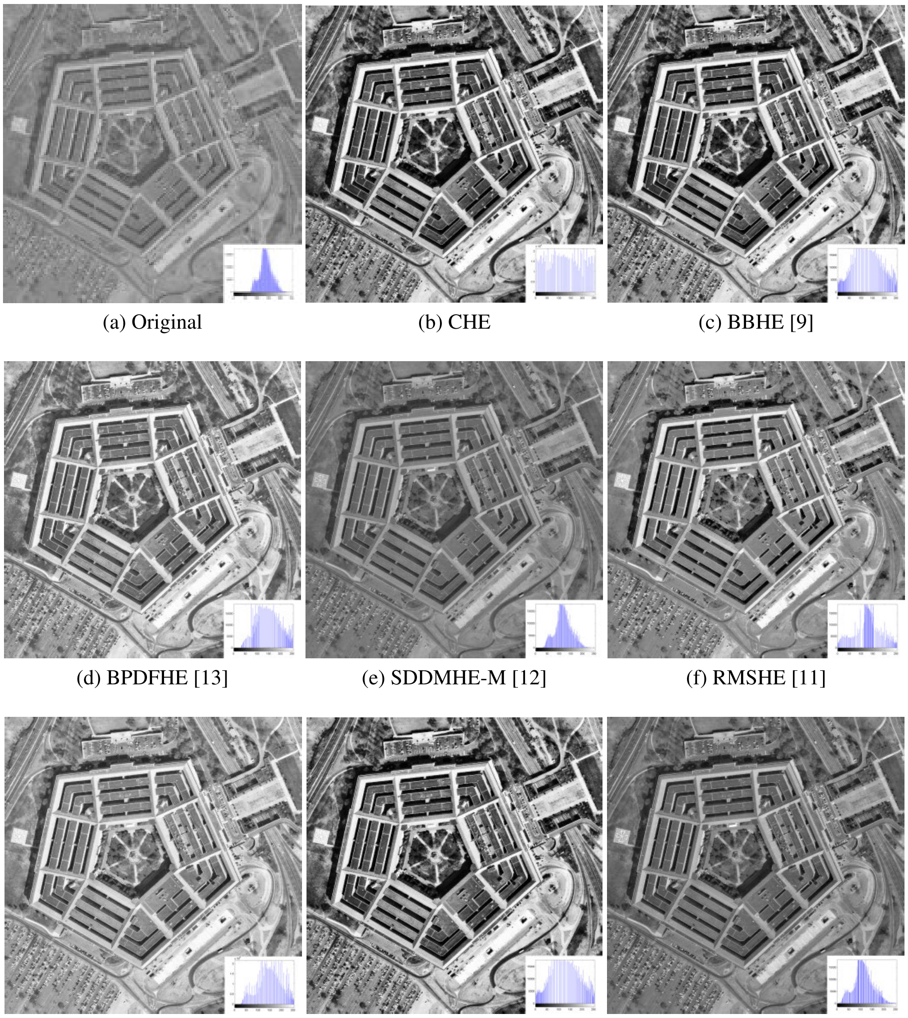

(a) Original (b) CHE (c) BBHE [9]

(d) BPDFHE [13] (e) SDDMHE-M [12] (f) RMSHE [11]

(g) BHEMHB [10] (h) Fuzzy segmented HE [8] (i) Proposed

FIGURE 3. Results of various HE methods for ID2 image with respective histograms with respect to original image.

(a) Original (b) $\mathbb{L}$* enhanced (c) V enhanced

FIGURE 4. Results of proposed method on transformed colour image.

methods. The high time complexity ($\mathbb{O}$) of the proposed method lies in expansion of each segment to full dynamic range using fuzzy expansion function and defuzzification of intensity levels, i.e. additional $\mathbb{O}(\eta_f L + \eta_d L)$ compared to classical multi-HE method (RMSHE), where η_f and η_d are bounded constant time procedure that adds up all elements of fuzzification and defuzzification functions respectively.

As stated earlier, the proposed method can easily be extended to the colour images, by transforming the RGB image to CIE $\mathbb{L} * a * b$ (or HSV) colour space. Then the

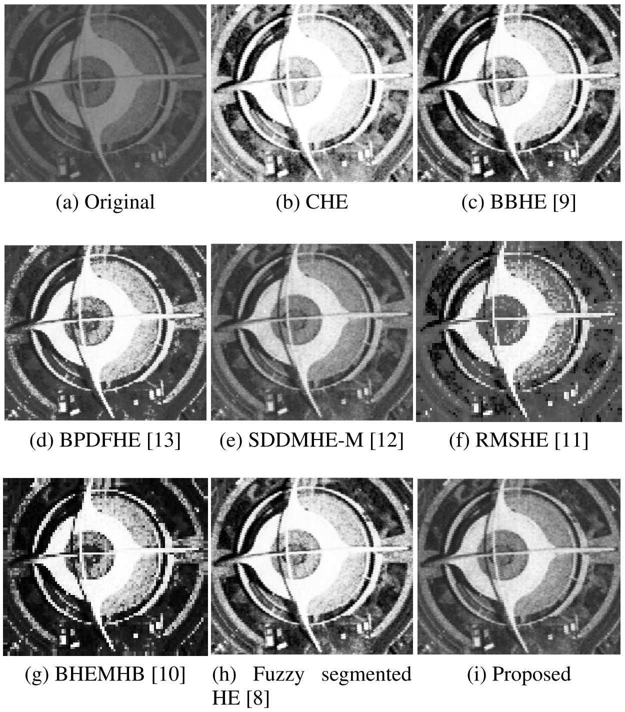

FIGURE 5. Zoom-in results of HE methods for a specific region in ID1 image (building in the top right) with respect to original image.

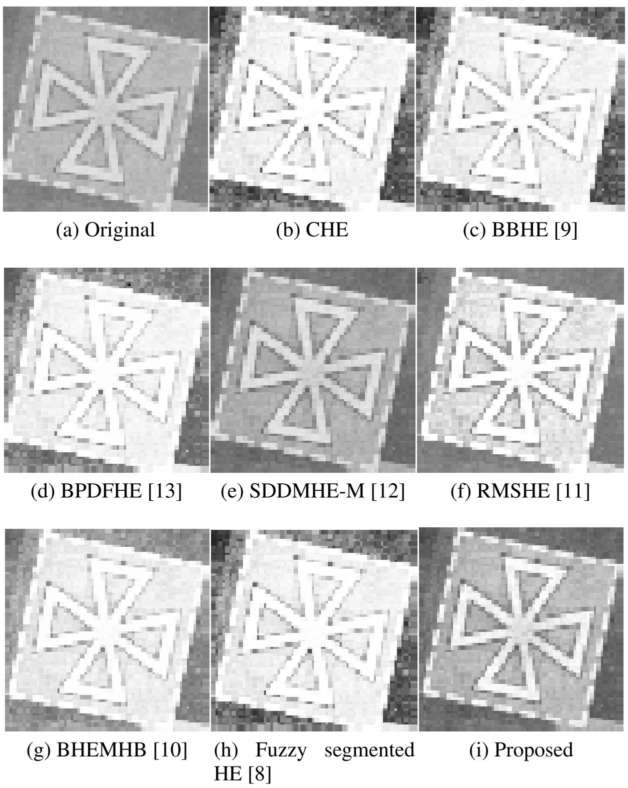

FIGURE 6. Zoom-in results of HE methods for a specific region in ID2 image (floral designed floor on the extreme left of the pentagon) with respect to original image.

luminance component $\mathbb{L}*$ (or V) is enhanced using proposed method, while conserving the chrominance components of the image. Finally, the inverse transformation is performed to obtain the output RGB image. Fig. 4 shows the contrast enhancement of the San Francisco (Golden Gate) image using proposed method. Observing Fig. 4 it can be stated that, application of proposed method on $\mathbb{L}*$ and V components enhances the image contrast without introducing any visual artifacts.

IV. CONCLUSION

In this paper, a novel fuzzy mapping based HE method has been proposed. The novelty of proposed method lies in the fuzzy scaling of each segment to the full range of intensities with help of fuzzy membership function, followed by the optimised normalisation process. To achieve artifact free contrast enhancement, the proposed method avoids un-even distribution of bins in the output image histogram, and utilises the dynamic range more efficiently during enhancement process. This has been achieved by fuzzifying the intensities of each sub-histogram to the full dynamic range. The simulation results show that the proposed method outperforms other contemporary methods for three metrics namely PSNR, *UIQ* and *R* used for average performance evaluation. Despite its effectiveness, the computational complexity of the proposed method is higher compare to conventional HE, but comparable to that of other methods. Reducing the computational complexity of proposed method is the objective of future research.

APPENDIX

Observing Fig. 5(a)-(i), it can be stated that, excessive saturation and un-even expansion of intensity bins by CHE, BBHE, BPDFHE, RMSHE, BHEMHB and Fuzzy segmented HE methods have introduced severe artifacts in the processed images. On the other hand, images processed by SDDMHE-M and proposed methods, have comparatively better results than contemporary HE methods. A close observation of Fig. 5(e) and (i) reveals that, the visual dynamic range of SDDMHE-M method is slightly lower than proposed method or the intensity of pixels surrounding the edges have smaller variance, that resulted into marginally reduced subjective clarity of the image processed by SDDMHE-M method. A similar behaviour has been observed in Fig. 6.

REFERENCES

[1] H. Demirel, C. Ozcinar, and G. Anbarjafari, “Satellite image contrast enhancement using discrete wavelet transform and singular value decomposition,” *IEEE Geosci. Remote Sens. Lett.*, vol. 7, no. 2, pp. 333–337, Apr. 2010.

[2] X. Fu, J. Wang, D. Zeng, Y. Huang, and X. Ding, “Remote sensing image enhancement using regularized-histogram equalization and DCT,” *IEEE Geosci. Remote Sens. Lett.*, vol. 12, no. 11, pp. 2301–2305, Nov. 2015.

[3] Y. Yuan, X. Zheng, and X. Lu, “Spectral–spatial kernel regularized for hyperspectral image denoising,” *IEEE Trans. Geosci. Remote Sens.*, vol. 53, no. 7, pp. 3815–3832, Jul. 2015.

[4] A. M. Chaudhry, M. M. Riaz, and A. Ghafoor, “A framework for outdoor RGB image enhancement and dehazing,” *IEEE Geosci. Remote Sens. Lett.*, vol. 15, no. 6, pp. 932–936, Jun. 2018.

[5] Y. Yuan, X. Zheng, and X. Lu, “Hyperspectral image superresolution by transfer learning,” *IEEE J. Sel. Topics Appl. Earth Observ. Remote Sens.*, vol. 10, no. 5, pp. 1963–1974, May 2017.

[6] Y. Yang, L. Wu, S. Huang, J. Sun, W. Wan, and J. Wu, "Compensation details-based injection model for remote sensing image fusion," *IEEE Geosci. Remote Sens. Lett.*, vol. 15, no. 5, pp. 734–738, May 2018.
[7] J. Liu, C. Zhou, P. Chen, and C. Kang, "An efficient contrast enhancement method for remote sensing images," *IEEE Geosci. Remote Sens. Lett.*, vol. 14, no. 10, pp. 1715–1719, Oct. 2017.
[8] M. F. Khan, D. Goyal, M. M. Nofal, E. Khan, R. Al-Hmouz, and E. Herrera-Viedma, "Fuzzy-based histogram partitioning for bi-histogram equalisation of low contrast images," *IEEE Access*, vol. 8, pp. 11595–11614, 2020.
[9] Y.-T. Kim, "Contrast enhancement using brightness preserving bi-histogram equalization," *IEEE Trans. Consum. Electron.*, vol. 43, no. 1, pp. 1–8, Feb. 1997.
[10] J. R. Tang and N. A. M. Isa, "Bi-histogram equalization using modified histogram bins," *Appl. Soft Comput.*, vol. 55, pp. 31–43, Jun. 2017.
[11] S.-D. Chen and A. R. Ramli, "Contrast enhancement using recursive mean-separate histogram equalization for scalable brightness preservation," *IEEE Trans. Consum. Electron.*, vol. 49, no. 4, pp. 1301–1309, Nov. 2003.
[12] M. F. Khan, E. Khan, and Z. A. Abbasi, "Segment dependent dynamic multi-histogram equalization for image contrast enhancement," *Digit. Signal Process.*, vol. 25, pp. 198–223, Feb. 2014.
[13] D. Sheet, H. Garud, A. Suveer, M. Mahadevappa, and J. Chatterjee, "Brightness preserving dynamic fuzzy histogram equalization," *IEEE Trans. Consum. Electron.*, vol. 56, no. 4, pp. 2475–2480, Nov. 2010.
[14] M. F. Khan, X. Ren, and E. Khan, "Semi dynamic fuzzy histogram equalization," *Optik*, vol. 126, no. 21, pp. 2848–2853, Nov. 2015.
[15] Z. Wang and A. C. Bovik, "A universal image quality index," *IEEE Signal Process. Lett.*, vol. 9, no. 3, pp. 81–84, Mar. 2002.
[16] E. Maggiori, Y. Tarabalka, G. Charpiat, and P. Alliez, "Can semantic labeling methods generalize to any city? The inria aerial image labeling benchmark," in *Proc. IEEE Int. Geosci. Remote Sens. Symp. (IGARSS)*, Jul. 2017, pp. 3226–3229.
[17] S.-D. Chen, "A new image quality measure for assessment of histogram equalization-based contrast enhancement techniques," *Digit. Signal Process.*, vol. 22, no. 4, pp. 640–647, Jul. 2012.

MOHAMMAD FARHAN KHAN received the B.Tech. and M.Tech. degrees in electronics engineering from the Z. H. College of Engineering and Technology, Aligarh Muslim University, India, in 2010 and 2012, respectively, and the Ph.D. degree in electronics engineering from the School of Engineering and Digital Arts, University of Kent, U.K., in 2017. He has worked as a Postdoctoral Research Associate of the EPSRC project that was in collaboration with the University of Warwick, U.K., and the University of Central Lancashire, U.K. His research interests include applied control theory, 2D/3D monitoring, image processing, mathematical modeling, soft computing, machine learning, artificial intelligence, and computational biology. He is acting as a Guest Editor of the special issue on the synergies of soft computing, artificial intelligence, and signal/image processing techniques in the advancement of sustainable technologies for *Sustainability* (MDPI), an SCIE journal.

EKRAM KHAN received the B.Sc.Eng. and M.Sc.Eng. degrees in electronics engineering from Aligarh Muslim University (AMU), Aligarh, India, in 1991 and 1994, respectively, and the Ph.D. degree in electronics engineering from the University of Essex, Colchester, U.K., in 2003. In 1993, he joined the Department of Electronics Engineering, AMU, where he has been a Professor, since 2009. He has successfully completed several research projects funded by various agencies in India and the U.K. He spent the summer at the University of Essex, as an Academic Visitor, in 2005 and 2006, funded by the Royal Society, U.K. He has authored or coauthored over 90 papers in refereed academic journals and international conference proceedings. His research interests include low-complexity image/video coding, video transmission over wireless networks, and biomedical image processing. He is also a Life Member of the Institution of Electronics and Telecommunication Engineers, India, and the Systems Society of India. He received the Commonwealth Scholarship to pursue the Ph.D. degree with the University of Essex. He also received the Research Award from the IBM T. J. Watson Research Laboratory, USA, for the best disruptive idea presented at the IEEE ICME 2002, held at EPFL, Switzerland.

MUAFFAQ M. NOFAL received the B.S. and M.S. degrees in physics from the University of Jordan, in 1991 and 1995, respectively, and the Ph.D. degree in experimental atomic physics from Frankfurt University, Germany, in 2007. From 2007 to 2009, he worked as an Assistant Professor with Applied Science University, Amman, Jordan. Since 2009, he has been an Assistant Professor with the Department of Science, Prince Sultan University, Saudi Arabia.

M. MURSALEEN has served as a Chairman of the Department of Mathematics, Aligarh Muslim University. He is currently a Principal Investigator of the SERB Core Research Project. He is also affiliated with China Medical University, Taichung, Taiwan. He has published nine books and more than 330 research articles in the fields of summability, sequence spaces, approximation theory, fixed point theory, and the measures of noncompactness. He has a number of academic visits in several countries and has successfully completed several national and international projects. Besides mentoring several master's degree students, he has guided twenty Ph.D. degree students. He was recognized as a Highly Cited Researcher by the Web of Science, in 2019. He is acting as a member of editorial boards of several international scientific journals and has also served as a reviewer for various international scientific journals.